

Influence of underground space development mode on the groundwater flow field in Xiong'an new area

Yi-hang Gao, Jun-hui Shen, Lin Chen, Xiao Li, Shuang Jin, Zhen Ma, Qing-hua Meng

Citation:

Gao YH, Shen JH, Chen L, *et al.* 2023. Influence of underground space development mode on the groundwater flow field in Xiong'an new area. *Journal of Groundwater Science and Engineering*, 11(1): 68-80.

View online: <https://doi.org/10.26599/JGSE.2023.9280007>

Articles you may be interested in

[Study on the geothermal production and reinjection mode in Xiong County](#)

Journal of Groundwater Science and Engineering. 2018, 6(3): 178-186 <https://doi.org/10.19637/j.cnki.2305-7068.2018.03.003>

[Pollution pattern of underground river in karst area of the Southwest China](#)

Journal of Groundwater Science and Engineering. 2018, 6(2): 71-83

[Influence of borehole quantity and distribution on lithology field simulation](#)

Journal of Groundwater Science and Engineering. 2019, 7(4): 295-308 <https://doi.org/DOI: 10.19637/j.cnki.2305-7068.2019.04.001>

[Numerical simulation of response of groundwater flow system in inland basin to density changes](#)

Journal of Groundwater Science and Engineering. 2018, 6(1): 7-17 <https://doi.org/10.19637/j.cnki.2305-7068.2018.01.002>

[Study on multiple induced polarization parameters in groundwater exploration in Bashang poverty alleviation area of Hebei Province, China](#)

Journal of Groundwater Science and Engineering. 2020, 8(3): 274-280 <https://doi.org/10.19637/j.cnki.2305-7068.2020.03.007>

[Characteristics of karst groundwater system in the northern basin of Laiyuan Spring area](#)

Journal of Groundwater Science and Engineering. 2018, 6(4): 261-269 <https://doi.org/10.19637/j.cnki.2305-7068.2018.04.002>

Influence of underground space development mode on the groundwater flow field in Xiong'an new area

Yi-hang Gao^{1,2,3}, Jun-hui Shen^{2,3*}, Lin Chen^{4*}, Xiao Li⁴, Shuang Jin⁵, Zhen Ma¹, Qing-hua Meng¹

¹ Tianjin Geological Survey Center, China Geological Survey, Tianjin 300000, China.

² State Key Laboratory of Geohazard Prevention and Geoenvironment Protection, Chengdu University of Technology, Chengdu 610059, China.

³ College of Environment and Civil Engineering, Chengdu University of Technology, Chengdu 610059, China.

⁴ Shenyang Geological Survey Center, China Geological Survey, Shenyang 110034, China.

⁵ Fifth Geological Brigade, Hebei Bureau of Geology and Mineral Resources, Tangshan 063000, Hebei Province, China.

Abstract: The degree and scale of underground space development are growing with the continuous advancement of urbanization in China. The lack of research on the change of the groundwater flow field before and after the development of underground space has led to various problems in the process of underground space development and operation. This paper took the key development zone of the Xiong'an New Area as the study area, and used the Groundwater modeling system software (GMS) to analyse the influence on the groundwater flow field under the point, line, and surface development modes. The main results showed that the underground space development would lead to the expansion and deepening of the cone of depression in the aquifer. The groundwater level on the upstream face of the underground structure would rise, while the water level on the downstream face would drop. The "line" concurrent development has the least impact on the groundwater flow field, and the maximum rise of water level on the upstream side of the underground structure is expected to be approximately 3.05 m. The "surface" development has the greatest impact on the groundwater flow field, and the maximum rise of water level is expected to be 7.17 m.

Keywords: Xiong'an new area; Groundwater flow field; Underground space; GMS

Received: 16 Jun 2022/ Accepted: 25 Nov 2022/ Published: 20 Mar 2023

Introduction

The degree and scale of underground space development are growing with the continuous advancement of urbanization in China. Urban densification leads to the construction of deeper structures (Bobylev, 2009) such as subways, building foundations, and underground car parks. At the same time, it also helps to alleviate the pressures of high population density, resource shortage, and environmental pollution in China (Chen et al. 2018; Li and Yuan, 2012). However, a series of problems caused by the development of underground spaces

have not been resolved, mainly including geotechnical engineering problems caused by groundwater (Serrano-Juan et al. 2018).

Groundwater is a crucial issue in the context of vertical urbanization. Research has suggested that groundwater rebound and decline would cause flooding and submergence of multiple underground structures and infrastructures (De Caro et al. 2020). Therefore, it is necessary to understand the characteristics of the groundwater flow field before and after underground space development and make precautionary preparations

Underground structures and groundwater are interdependent on each other. Groundwater flow (Attard et al. 2016; Xu et al. 2013), quality (Chandrasekharan et al. 2005), and temperature (Hu et al. 2008) can vary with the development of the underground structures, while underground structures can be greatly impacted by these changes. The presence of underground structures blocks the normal flow path and state of groundwater and forces it to change its original state. In

*Corresponding author: Jun-hui Shen, Lin Chen, E-mail address: shenjinhui@cdut.cn 392446434@qq.com

DOI: [10.26599/JGSE.2023.9280007](https://doi.org/10.26599/JGSE.2023.9280007)

Gao YH, Shen JH, Chen L, et al. 2023. Influence of underground space development mode on the groundwater flow field in Xiong'an new area. Journal of Groundwater Science and Engineering, 11(1): 68-80.

2305-7068/© 2023 Journal of Groundwater Science and Engineering Editorial Office This is an open access article under the CC BY-NC-ND license (<http://creativecommons.org/licenses/by-nc-nd/4.0>)

particular, during large-scale underground development, the influence cannot be ignored (Paris et al. 2010; Ricci et al. 2007). The changes in the groundwater system frequently cause the deformation and reduced strength of rock and soil, which may develop to geological disasters (Wu, 2003).

The development mode of underground space can be divided into “point”, “linear” and “surface”, in which “surface” is a combination of the former two. At present, it is concluded that each development mode can influence the groundwater flow field, but the comparative study of the three modes has not been conducted yet.

Xu et al. (2012) analyzed the effects of underground structures on land subsidence and studied the blocking effect of underground structures on groundwater flow through laboratory tests and numerical simulations. Attard et al. (2017) investigated the impact of underground structures on the intrinsic vulnerability of urban aquifers. De Caro et al. (2020) simulated the interaction between underground structures and groundwater in the city of Milan. The results show that significant modifications of groundwater head distribution are observed when underground structures transversally cut the groundwater flow, resulting in the fragmentation of the groundwater flow pathways, leading to changes in the groundwater head.

On April 1th 2017, the Central Committee of the Communist Party of China and the State Council decided to establish the Xiong’an New Area of Hebei Province, aiming to build a world-class green modern smart city with a high starting point and standards (Li et al. 2020; Wang et al. 2021). Large-scale underground space construction will inevitably block groundwater runoff and change its original path, thus triggering a series of geological problems. In this study, based on the planned location of underground space in the Xiong’an New Area, the influence of three development modes of “point”, “line” and “surface” on the groundwater flow field during the process of foundation pit excavation and operation is simulated. The objectives of this study are: (1) to establish the shallow groundwater flow model; (2) to compare the influence of three modes of underground space development and utilization on shallow groundwater flow fields and (3) to provide reasonable suggestions for the development of underground space in the Xiong’an New Area.

1 General characteristics of the study area

The Xiong’an New Area is located in the hinterland of Beijing, Tianjin, and Baoding in the central part of Hebei Plain, and includes Xiong County, Anxin County, and Rongcheng County. The Xiong’an New Area belongs to a warm temperate continental monsoon climate with four seasons and has an average temperature of 12.1 °C, and an average annual precipitation of 560 mm (Wang et al. 2021; Xie et al. 2019; Xu et al. 2018).

The study area is located in the northern part of Xiong’an New Area, mainly Rongcheng County and some surrounding areas (Fig. 1). The terrain gradually descends from the northwest to the southeast. The elevation is mostly in the range of 5–26 m, and the terrain is relatively flat with less than 2 ‰ of gradient. According to the study area genetic type and surface morphology, it can be further classified into subareas as alluvial flood plains, alluvial lacustrine plains, and alluvial plains, in which the alluvial plain is only distributed locally to the southern boundary. The uppermost Quaternary sediments are generally loose with a thickness of 300 m and are mainly alluvial, pluvial, and lacustrine silty clay, silt, and sandy silt (Foster et al. 2004).

According to the statistics of numerous boreholes and aquifer lithology in the study area (He et al. 2018; Liu et al. 2009; Ma et al. 2020), the grain size of the Quaternary sediments varies from fine to coarse and then to finer from top to bottom, which constitutes a relatively complete sedimentary cycle. It reflects the evolution process of runoff since the Quaternary period, from weak to strong and then to weaker. All the Quaternary series of this area show significant rhythmic cycling changes. Except for the alluvial pluvial fans in front of the mountains, the clayey soil in the middle and upper strata of each series is rich in the rest of the areas, and the thickness varies from 6 m to 25 m. Such hydrogeological setting forms a relatively stable confining bed, while the middle and lower aquifers are abundant and coarser, resulting in an independent secondary water-bearing system. Therefore, based on the lithology of Quaternary sediments, we can divide the loose deposits in the study area into four aquifer groups from top to bottom, according to their hydraulic properties and the vertical distribution of aquifers and confining beds (Fig. 1). Groundwater in Aquifer Groups I and II is defined as shallow groundwater, whereas Aquifer Groups III and IV contain deep groundwater. Because the thickness of the first group is small, it is rarely exploited alone. There is a close hydraulic connection between the first and the second aquifer groups and they can be considered a unified water-bearing body which is the main exploitation target of the area. It has a significant

exploitation target of the area. It has a significant

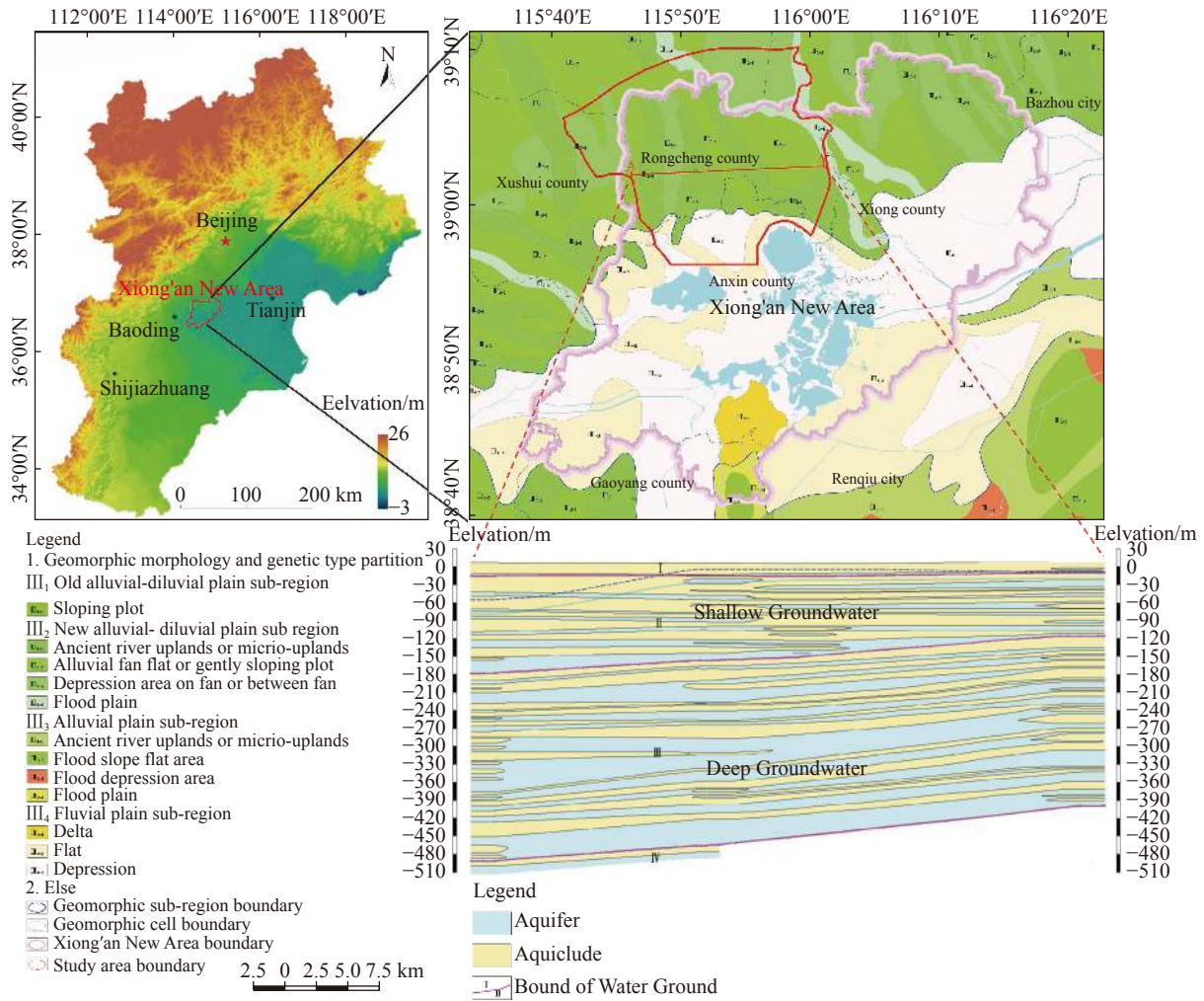


Fig. 1 Geomorphological map and typical profile of the study area

influence on the development of underground space in the study area (Chi et al. 2021; Zhu et al. 2022; Li et al. 2017; Qin et al. 2013).

2 Model construction

2.1 Hydrogeological conceptual model

This study area takes the river and contour line of hydraulic head as its boundary, and includes the underground space development layers and the confined aquifer that may be affected in the lower part. The aquifer lithology is dominated by fine sand, silt, and medium sand with coarse sand locally. The final model layers include five unsaturated zones, one unconfined aquifer, five confined aquifers, one low-permeability aquifer, and six impermeable layers, and the stratum and lithology of each layer were shown in Table 1. The data from the drilling works were processed and the base map were verified to ensure that each borehole site shown on the base map matches the

drilling data. In this study, 188 boreholes were used, and a three-dimensional geological model with a shallow depth of 100 m in an area of 560 km² was constructed. Moreover, the distribution condition of the stratigraphy within the depth of 50 m of the unground space and its influence on the regional groundwater seepage field were studied.

There is a close hydraulic connection between the different aquifer layers; thus, sandy layers were selected as the target aquifers. The aquifers are generalized into a heterogeneous anisotropic porous medium, according to the strata characteristics framed by sedimentology (Borgia et al. 2011; Mengistu et al. 2019; Sathe and Mahanta, 2019). For calibration purpose, we collected observation data of the groundwater level and comprehensively analyzed the groundwater flow field. We then conceptualized the groundwater flow of the target layers as a three-dimensional transient flow system.

2.2 Formulating the numerical model

A three-dimensional numerical model with hetero-

Table 1 Initial hydraulic properties

No.	Stratum and lithology	Layer	Horizontal hydraulic conductivity (m/d)	Vertical hydraulic conductivity (m/d)	Specific yield
1	Landfill	Unsaturated zone	8.35e-05	3.77e-05	0.027 5
2	Alluvial pluvial soil	Unsaturated zone	2.3e-03	7.4e-03	0.027 5
3	Alluvial lacustrine soil	Unsaturated zone	5.1e-03	7.6e-03	0.027 5
4	Clay + silt	Unsaturated zone	3.0e-03	5.9e-03	0.037 5
5	Clayey sand	Unsaturated zone	1.0e-04	1.6e-04	0.037 5
6	Find sand + silt	Unconfined aquifer	3.16	3.16	0.04
7	Clay + silt	Low-permeability aquifer	9.5e-03	7.30e-03	0.037 5
8	Find sand + silt	Confined aquifer	0.907	0.907	0.047 5
9	Clayey soil	Impermeable layer	1.0e-04	1.6e-04	0.027 5
10	Find sand + Silt + Medium sand	Confined aquifer	0.777 6	0.777 6	0.07
11	Clayey soil	Impermeable layer	2.8e-03	3.9e-04	0.027 5
12	Clayey soil	Impermeable layer	2.1e-04	3.2e-04	0.027 5
13	Find sand + Silt + Medium sand	Confined aquifer	2.592	2.592	0.095
14	Clayey soil	Impermeable layer	1.5e-02	3.7e-03	0.027 5
15	Find sand + Medium sand	Confined aquifer	2.592	2.592	0.095
16	Clayey soil	Impermeable layer	8.5e-05	1.6e-04	0.027 5
17	Find sand + Medium sand	Confined aquifer	2.592	2.592	0.095
18	Clayey soil	Impermeable layer	1.9e-04	3.6e-04	0.027 5

geneous anisotropy and transient flow (Equation(1)) in the study area was established; this model uses Darcy’s law and continuity principle to model the hydrogeological conditions of the study area.

$$\left\{ \begin{array}{l} \frac{\partial}{\partial x} \left(K_{xx} \frac{\partial h}{\partial x} \right) + \frac{\partial}{\partial y} \left(K_{yy} \frac{\partial h}{\partial y} \right) + \frac{\partial}{\partial z} \left(K_{zz} \frac{\partial h}{\partial z} \right) + \varepsilon = \\ S_s \frac{\partial h}{\partial t}, (x, y, z) \in \Omega, t \geq 0 \\ h(x, y, z, t)|_{t=0} = h_0(x, y, z) \in \Omega \\ h(x, y, z, t)|_{\Gamma_1} = h_1(x, y, z, t), (x, y, z) \in \Gamma_1, t \geq 0 \\ K \frac{\partial h}{\partial n} |_{\Gamma_2} = q(x, y, z, t), (x, y, z) \in \Gamma_2, t \geq 0 \end{array} \right. \quad (1)$$

Where: K_{xx} and K_{yy} are the horizontal hydraulic conductivities (m/d); K_{zz} is the vertical hydraulic conductivity (m/d); S_s is the specific storage (m^{-1}); Ω is the seepage area; h_1 is the hydraulic head on the Type 1 boundary conditions (m); K_n is hydraulic conductivity along the normal direction of the Type 2 boundary (m/d); q is the flow rate on the second type of boundary conditions (m^3/d); h is the hydraulic head (m); ε is the source and sink items (d^{-1}); t is the time (s); h_0 is the initial water level (m); Γ_1 is the first type of boundary condition; Γ_2 is the second type of boundary condition.

2.3 Boundary conditions and parameters

The northern part of the model consisted of a flow boundary. Based on the hydraulic gradient determined by the groundwater level in the boreholes, the flow rate is calculated according to Darcy’s law. The southern and eastern boundaries are the Type 2 boundary associated with the average state of rivers, lakes, and depressions. The western boundary is a no-flow boundary. The upper boundary is the phreatic water table, which is the water exchange boundary with changing positions and is also affected by rainfall infiltration and artificial pumping. The lower boundary is silty clay at a depth of 100 m and is conceptualized as an impervious bottom. The entire study area has a moderate permeability, and the unsaturated zone is mainly composed of sand and silt, which is extensively distributed throughout the plain areas, and the average infiltration coefficient of precipitation is 0.221 5 (Wang et al. 2010).

According to the urban development objectives and geological conditions in the study area, the underground space development areas can be divided into prohibited construction areas, reserve areas, key development areas, and suitable construction areas (Cui et al. 2021; Qiao and Peng,

2016). A suitable construction area with a larger extent can be developed with the “surface” mode; the linear works in the suitable construction area can be developed with the “line” mode; the key development area is relatively limited and can be developed with a “point” mode. The location of the underground space is determined according to the engineering plan, and refined in the model mesh to meet the modeling requirements. The unit is taken as an impervious medium, and the hydraulic conductivity is 10^{-10} m/s in the analysis.

The initial hydraulic property values adopted for this calculation include the hydraulic conductivity, specific yield of each layer at the heights of the river heads. These parameter values are listed in Table 1. The initial groundwater level is the groundwater level in the study area during the high-water period.

2.4 Construction of three-dimensional groundwater model

GMS software was used to build a three-dimensional groundwater model in the study area, and the response of the groundwater flow field to underground development was studied. The borehole module in the GMS software can use borehole data to build a solid model (Ma et al. 2019). A total of 188 borehole data were selected in the study area, of which the spacing of boreholes in the starting area was 500 m×500 m, and the spacing of boreholes in other areas was 1 000 m×1 000 m which could meet the research requirements for precision (Fig. 2).

2.5 Verification of the model

The identification and verification of the model is

an indispensable step to ensure that the model accurately reflects the characteristics of the groundwater flow field in the study area. Thus, the trial-and-error method (Chen et al. 2020; Han et al. 2016) and root mean square error (RMSE) (Makungo and Odiyo, 2017; Rwanga and Ndambuki, 2020; Singha et al. 2020; Uddin et al. 2018) were used to adjust the model. The Nash-Sutcliffe efficiency coefficient (NSE) (Makungo and Odiyo, 2017; Melaku and Wang, 2019) is often used to evaluate the simulated goodness of hydrological models, and its formula is given in Equation (2):

$$NSE = 1 - \frac{\sum_{i=1}^N (S_i - C_i)^2}{\sum_{i=1}^N (C_i - \bar{C})^2} \quad (2)$$

Where: S_i is the simulation value; \bar{C} is the average of all the measured values; C_i is the measured value.

The value range of NSE is $-\infty$ to 1, and the closer the value is to 1, the more reliable the simulation result is. The simulated NSE is 0.903, proving the reliability of the simulation results (Zou et al. 2021).

The RMSE is the square root of the ratio of the square of the calculated value to the measured value and the ratio n of the sample number (Dong and Zhang, 2021; Li et al. 2021; Yang et al. 2021). The calculation formula is given in Equation (3). The root mean square error is very sensitive to the maximum or minimum error response in each set of calculations, so this method can accurately reflect the reliability of the simulation results (Yang and Zhang, 2021).

$$RMSE = \sqrt{\sum (C - C_p)^2 / N} \quad (3)$$

Where: C is the measured values; C_p is the calculated values; N is the number of samples.

The results of this simulation show a linear

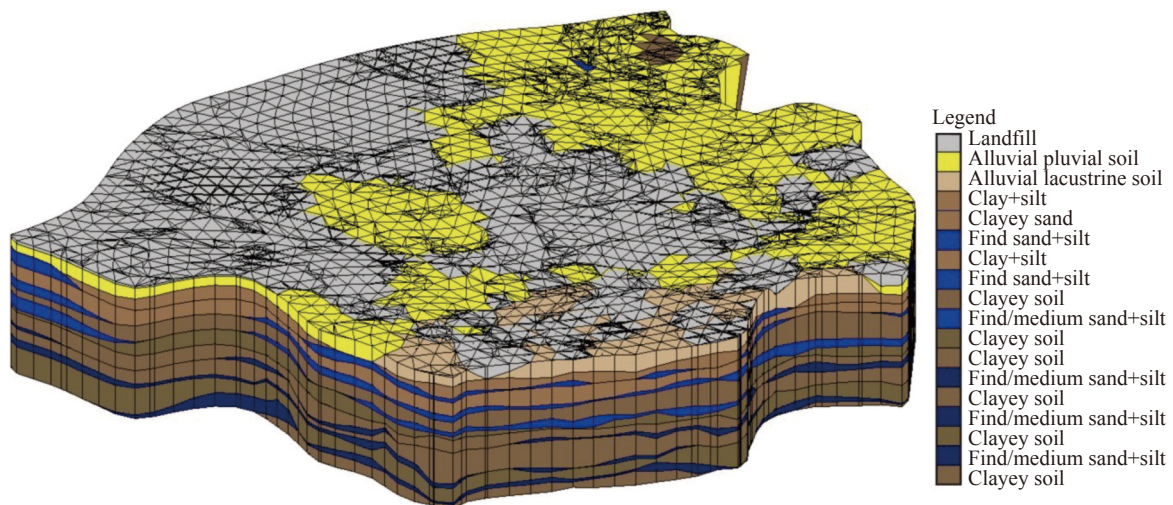


Fig. 2 Three-dimensional structure model of aquifer in the study area

relationship between the measured and calculated values with a slope of 1.020 4 ($R^2=0.931 3$) (Fig. 3). The RMSE of the 188 measured water levels in the study area was 1.14, indicating that the overall estimation effect of the model was reliable. Therefore, the model can be used to simulate the groundwater flow field in an area.

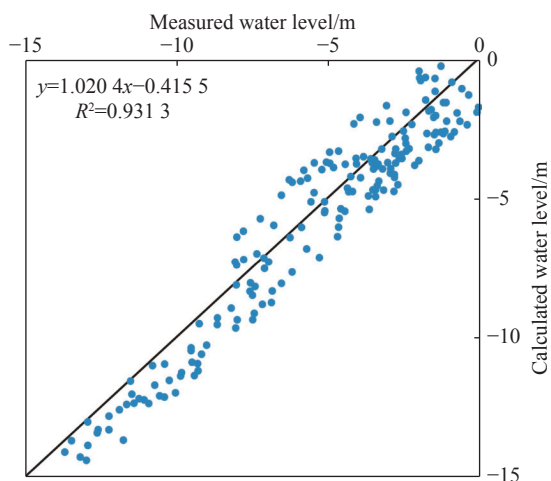


Fig. 3 Comparison of goodness of fit between the measured and calculated values

Because the measured values are affected by atmospheric rainfall and other factors, some individual observations are quite different from the simulated values, but they do not affect the overall simulation results of the model. In summary, it can be considered that the model can accurately reflect the actual situation of the underground aquifers in the study area, so we can consider that the model operation is stable, reliable, and can be used for predictive analysis.

3 Results and discussion

3.1 The influence of “point” underground space development on the groundwater flow field in fine sand

As shown in Fig. 4, the groundwater flow field was modelled prior to the underground space development. Fig. 5a shows the simulation result under the “point” underground development mode. Overall, after the development, except for the area near Baiyangdian, the groundwater level has generally

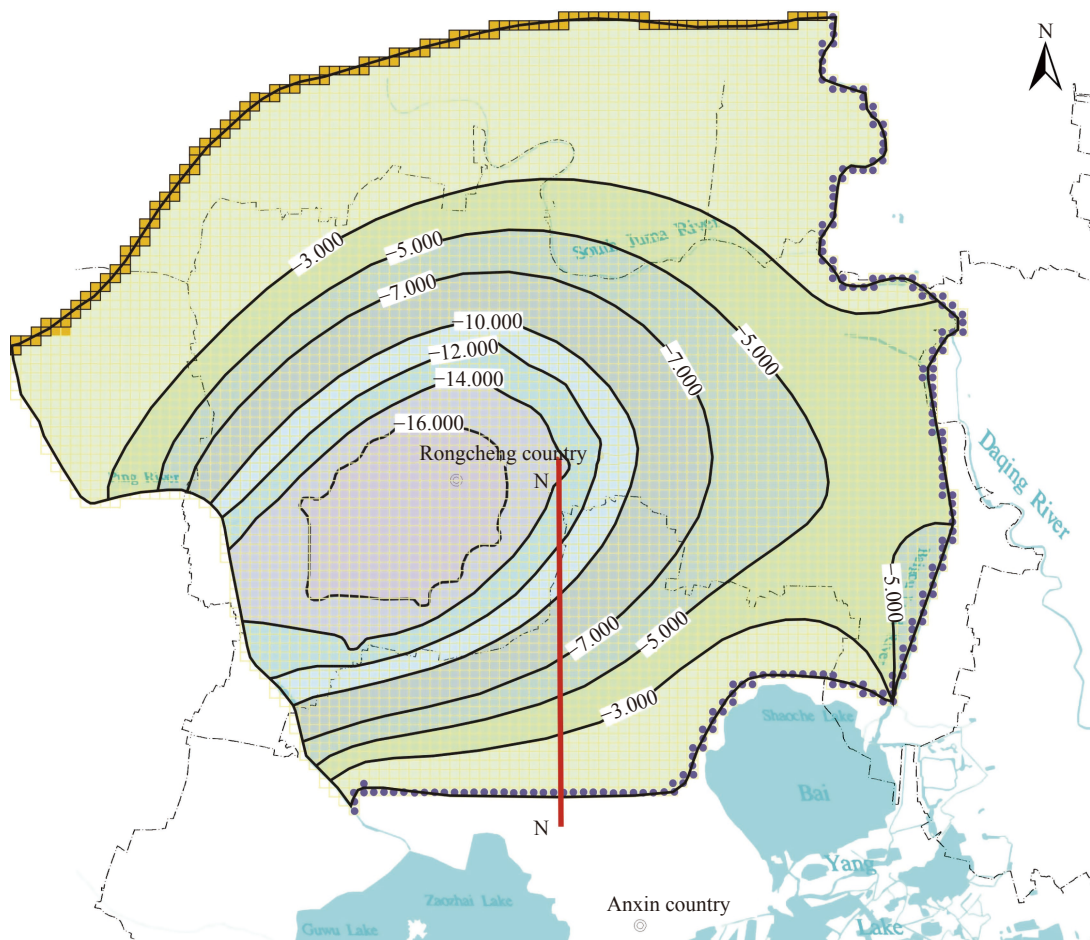


Fig. 4 Simulated groundwater levels prior to the development of the underground space

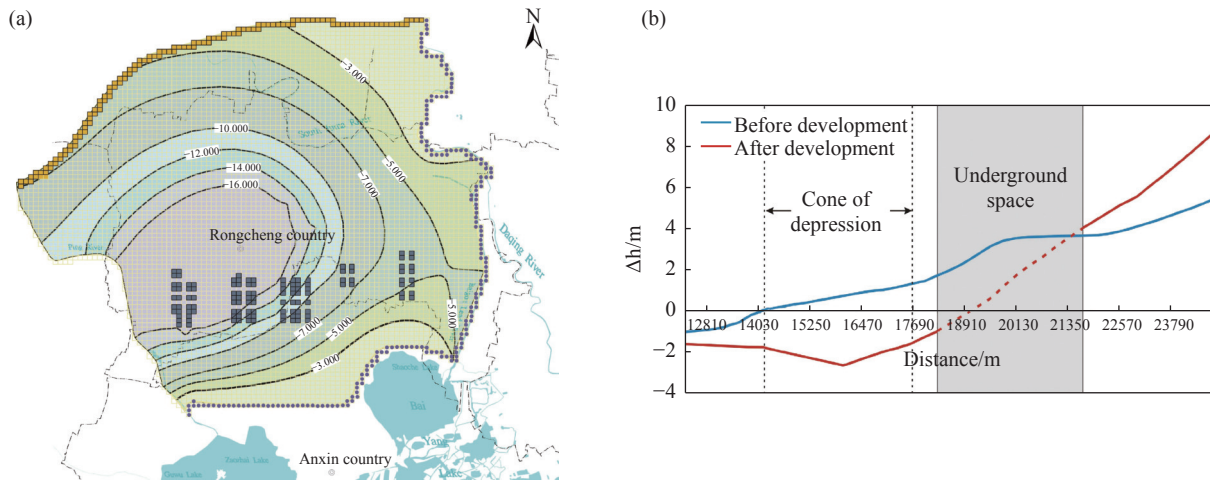


Fig. 5 a) Simulated groundwater levels in the “point” underground space development and b) profile of the groundwater level change in the “point” underground space (N-N Section)

declined, the extent of the cone of depression has significantly expanded, and the water level at the center of the cone has dropped by 3.92 m. In the northern part of the study area, although the groundwater level declined by 3–4 m, the hydraulic gradient in the same area did not change significantly. In the eastern part of the study area, because the regional groundwater flow direction is from northwest to southeast, the “point” underground space development will still block the original flowing path of groundwater. Furthermore, two separate areas which are located within 5 m water table contours on the east side of the underground space prior to development, are merged due to the expansion of depression after the development. In the southern part of the study area, groundwater level is not changed entirely, but it can be seen that there is an increase in groundwater contour in the same area, indicating that the hydraulic gradient has increased, and the maximum variation exceeds 5.45 m (Fig. 5a).

Although groundwater in the study area generally follows a northwest to southeast direction, the simulated underground space is located near Baiyangdian. The Baiyangdian depression is recharged by the surrounding groundwater, so the south side of the underground space can be regarded as the upstream face and the north side as the downstream face. Fig. 5a illustrates that the groundwater level rises slightly on the upstream side or the southern part of the underground project, and the maximum height is 3.50 m. A decline in groundwater level can be observed on the downstream side or the northern part, with a maximum drop of 3.60 m.

A profile of the groundwater level change under the “point” underground space development is

shown in Fig. 5b. It shows that the distribution of the groundwater level in the section is almost the same as the original water level. However, due to the blocking effect of the underground structure, the water level on the upstream face rises and is higher than the original water table, with an average increase of 1.81 m and a maximum of 3.24 m. The water level on the downstream face is lower than the original, with an average decrease of 2.19 m and a maximum of 3.34 m. The change in groundwater level is in the range of 4.0 km from the downstream face to the underground structure. In this section, the extent of the depression zone has expanded by approximately 3.4 km, and water level at the center has dropped by 3.34 m. After the completion of the underground structure, the hydraulic gradient on both the upstream and downstream faces has increased by 3.025 compared with the original hydraulic gradient.

3.2 Influence of the development of “line” underground space on the groundwater flow field in fine sand

Fig. 6a shows the simulation result under the “line” concurrent underground development. After the development, the depth to groundwater in the depression zone has slightly increased to 3.13 m, and the extent is expanded. In the southern part of the underground space near Baiyangdian, a slight rise in water level of approximately 3.05 m has occurred; the water level on the north side of the underground space has declined, with a reduction of 3.47 m. The southern water level counters are slightly denser, indicating that the hydraulic gradient in this area has increased.

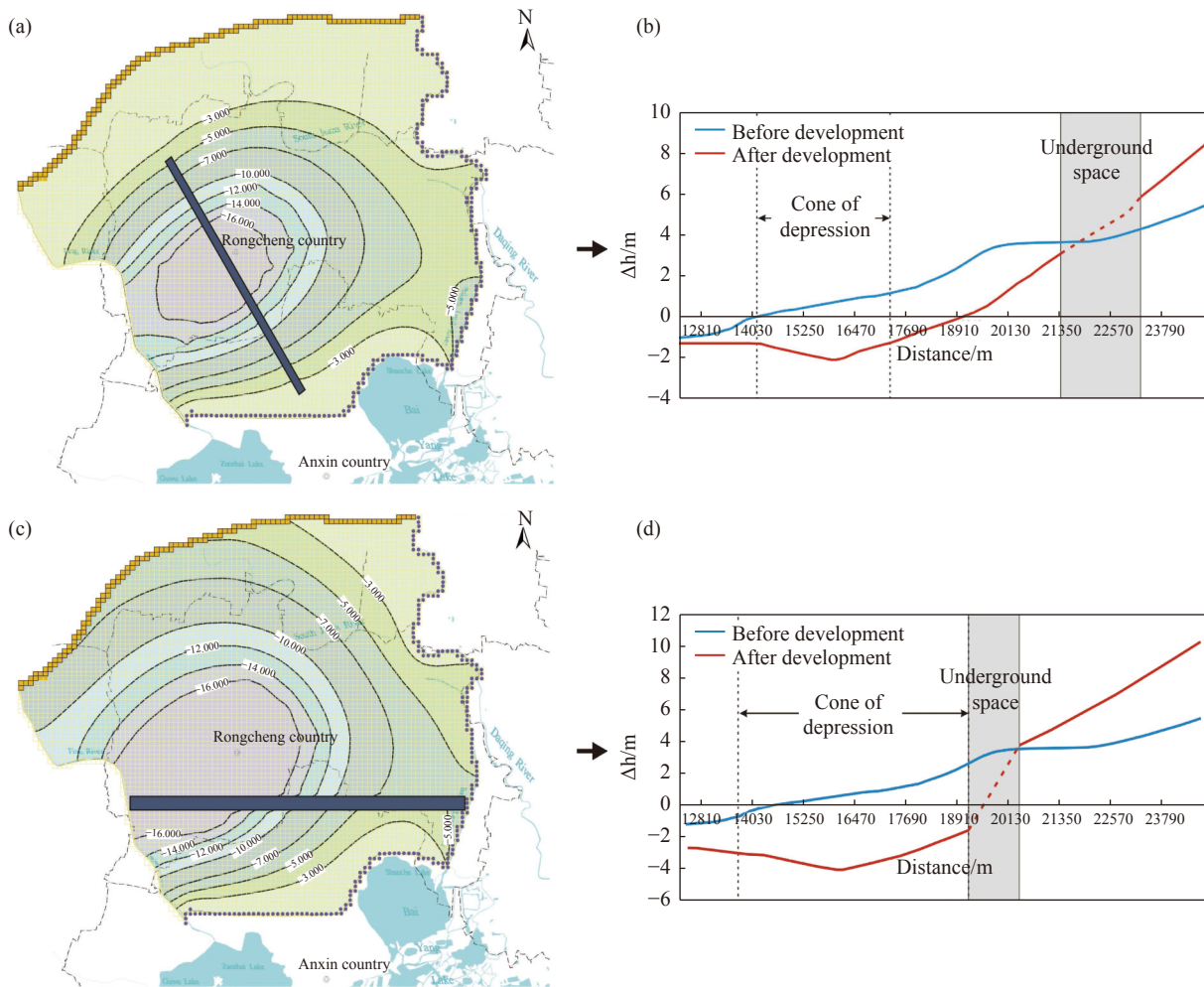


Fig. 6 Simulated groundwater levels in the a) “line” concurrent and c) “line” interception underground space development; Profile of the groundwater level change of the b) “line” concurrent and d) “line” interception underground space development (N-N Section)

A profile of the groundwater level change of the “line” concurrent underground space development is shown in Fig. 6b. It shows that the groundwater level distribution in this section is almost the same as the original. However, due to the blocking effect of the underground structure, the water level on the upstream of the structure rises higher than the original water table, with an average increase of 1.64 m and a maximum of 3.04 m. The water level on the downstream face is lower than the original, with an average decrease of 2.00 m and a maximum of 2.84 m. The groundwater level in the downstream face with a noticeable change is within 7.0 km from the underground structure. In this section, the extent of the descending funnel has expanded by 3.0 km, and water level at the center has dropped by 2.84 m. After completion of the underground structure, the hydraulic gradient on both the upstream and downstream faces has increased by 2.01 compared with the original hydraulic gradient.

In contrast, the impact of the “line” interception on the groundwater flow field is much larger (Fig. 6c). First, groundwater level has generally declined. Before development, the 5 m contour lines of water level in the east occurred in two separated areas; after the development, they have merged into a single area. Second, the extent of the descending zone was expanded, and the water level at the center has decreased by 5.04 m. Although the groundwater level in the south of the underground project has also declined, there is an abrupt groundwater level change within an area of 0.5 km of the underground works, which is close to the upstream of the underground project. Groundwater level has risen with a maximum increase of 5.30 m. On the downstream face or the north side, around 480 m from the construction, a significant groundwater level decline of up to 4.95 m can be identified.

Fig. 6d is a profile of the groundwater level variations in underground space development un-

der the condition of “line” interception. The water level distribution along the section is generally the same as that of the original. However, due to the blocking effect of the underground structure, the water level generally rises, with an average increase of 2.73 m and a maximum of 4.85 m. The water level on the downstream face has dropped below the original with an average decrease of 3.39 m and a maximum decrease of 4.74 m. The impacted area is around 5.8 km from the underground structure the downstream face. Along this section, the extent of the depression zone has expanded by approximately 5.5 km, and the water level decline at the depression center is 4.75 m. After completion of the underground structure, the hydraulic gradient on both the upstream and downstream faces has increased by 3.92 compared with the original hydraulic gradient.

3.3 Influence of the “surface” underground space development on the groundwater flow field in fine sand

Fig. 7 shows the simulation result under the “surface” underground development mode. The construction of the “surface” underground works has greatly influenced the groundwater flow field. First, the depth of the groundwater level in the study area has generally increased. Before the development, the 5 m contour lines of water level in the east occurred in two separated areas; after the development, they have merged into a single area. Secondly, the extent of the depression zone has expanded, and the water level at the center has dropped more than 8.00 m. Thirdly, although the groundwater level on the upstream/south side of

the underground works has dropped, there is a sudden water level change within 1 km of underground works, which is shown as being close to the upstream side of the underground project. The groundwater level has increased, with a maximum of 7.17 m (Fig. 7a). There is also a significant change on the downstream face or the north side around 0.6 km from the project site. The groundwater level has dropped by up to 7.67 m on the downstream side of the underground works.

It can be seen from the profile of the groundwater level variation in the “surface” underground space development that the groundwater level distribution is generally the same as that of the original (Fig. 7b). Because of the blocking effect of the underground structure, the upstream water level has increased with an average of 4.76 m and a maximum of 6.67 m. However, on the downstream side, the water level has dropped with an average decrease of 4.69 m and a maximum of 7.17 m. The impacted area of the development of underground structures exceeds 8 km in the north from the construction site. In this section, the extent of the depression zone has expanded up to 7.7 km, and the water level at the center has dropped 6.96 m. After completion of the project, the hydraulic gradient on both the upstream and downstream faces has increased by 12.82 compared with the original hydraulic gradient. The influences exerted by different modes of underground space development on the whole study area are listed in Table 2, along with the influences captured in the typical N-N section.

4 Conclusion

From the above descriptions, the blocking effect of

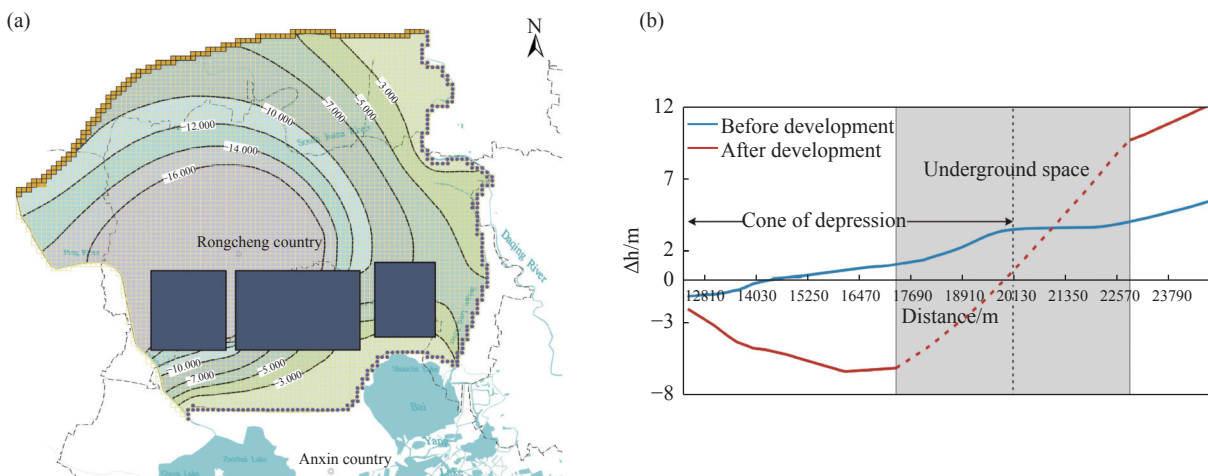


Fig. 7 a) Simulated groundwater levels in the “surface” underground space development and b) profile of groundwater level variation in the “surface” underground space development (N-N Section)

Table 2 List of data of the influences on groundwater exerted by different modes of underground space development

Development modes	Increasing amplitude (m)		Average (m)	Decreasing amplitude (m)		Average (m)
	Overall	N-N Section	N-N Section	Overall	N-N Section	N-N Section
Point	3.5	3.24	1.81	3.6	3.34	2.19
Line-down-flow	3.05	3.04	1.64	3.47	2.84	2
Line-cross-closure	5.3	4.85	2.73	4.95	4.74	3.39
Surface	7.17	6.67	4.76	7.67	7.17	4.69

Development modes	Funnel extent (km)	Decreasing amplitude in the center (m)		Hydraulic gradient		Extent of influence (km)
	N-N Section	Overall	N-N Section	Overall	N-N Section	N-N Section
Point	3.40	3.92	3.34	5.45	3.03	4.00
Line-down-flow	3.00	3.13	2.84	4.81	2.01	7.00
Line-cross-closure	5.50	5.04	4.75	8.33	3.92	5.80
Surface	7.70	>8	6.96	13.46	12.82	>8

underground structures, regardless of the mode of underground space development, has always led to an increase in the groundwater level in the upstream face and a decline in the downstream face. The area of the depression zone has expanded, and water level at the center has declined. The hydraulic gradients on both the upstream and downstream faces sides of the underground structures have increased to a certain degree compared with the original gradient.

The biggest impact on the groundwater flow field caused by the blocking effect of underground works is with the “surface” development mode, followed by the “line” interception mode, and the “point” mode, while the “line” concurrent development mode has the least effect on the groundwater flow field. Compared with the “line” concurrent development mode, the groundwater level on the upstream face of the underground structure under “surface” development mode has risen by 2.4 times, the maximum decline in the downstream face has increased by 2.2 times, the water level decline at the center of the depression has increased by 2.6 times, and the hydraulic gradient on both the upstream and downstream faces has increased by 2.8 times.

The influencing distance of the “surface” development mode on groundwater is the largest, followed by the “line” concurrent mode and then the “line” interception mode, while the “point” mode is the smallest. The influencing distance of the “surface” mode on groundwater is more than twice as much as that of the “point” mode. Therefore, when planning the underground space development mode and scale of the Xiong’an New Area, one should fully consider its overall impact and influence on groundwater to ensure the safety of

construction of underground structures and their operation.

Acknowledgements

This work was supported by the Evaluation of soil and water quality and engineering geological survey in Xiong’an New Area Program of China (Grant No. DD20189122), National Natural Science Foundation of China (Grant No. 42102294).

References

- Attard G, Rossier Y, Eisenlohr L. 2017. Underground structures increasing the intrinsic vulnerability of urban groundwater: Sensitivity analysis and development of an empirical law based on a groundwater age modelling approach. *Journal of Hydrology*, 552: 460–473. DOI: [10.1016/j.jhydrol.2017.07.013](https://doi.org/10.1016/j.jhydrol.2017.07.013).
- Attard G, Winiarski T, Rossier Y, et al. 2016. Review: Impact of underground structures on the flow of urban groundwater. *Hydrogeology Journal*, 24: 5–19. DOI: [10.1007/s10040-015-1317-3](https://doi.org/10.1007/s10040-015-1317-3).
- Bobylev N. 2009. Mainstreaming sustainable development into a city’s Master plan: A case of Urban Underground Space use. *Land Use Policy*, 26: 1128–1137. DOI: [10.1016/j.landusepol.2009.02.003](https://doi.org/10.1016/j.landusepol.2009.02.003).
- Borgia A, Cattaneo L, Marconi D, et al. 2011. Using a MODFLOW grid, generated with GMS, to solve a transport problem with TOUGH2 in complex geological environments: The inter-

- tidal deposits of the Venetian Lagoon. *Computers & Geosciences*, 37: 783–790. DOI: [10.1016/j.cageo.2010.11.007](https://doi.org/10.1016/j.cageo.2010.11.007).
- Chandrasekharan H, Tadi SG, Sarangi A, et al. 2005. Urbanization effects on the groundwater status of Delhi, India. In: Savic DA, Marino MA, Savenije HG, Bertoni JC, editors. *Sustainable Water Management Solutions for Large Cities*: 293, 294-298.
- Chen Y, Liu G, Huang X, et al. 2020. Development of a surrogate method of groundwater modeling using gated recurrent unit to improve the efficiency of parameter auto-calibration and global sensitivity analysis. *Journal of Hydrology*: 125726. DOI: [10.1016/j.jhydrol.2020.125726](https://doi.org/10.1016/j.jhydrol.2020.125726).
- Chen ZL, Chen JY, Liu H, et al. 2018. Present status and development trends of underground space in Chinese cities: Evaluation and analysis. *Tunnelling and Underground Space Technology*, 71: 253–270. (in Chinese) DOI: [10.1016/j.tust.2017.08.027](https://doi.org/10.1016/j.tust.2017.08.027).
- Chi G, Su X, Lyu H, et al. 2021. Simulating the shallow groundwater level response to artificial recharge and storage in the Plain area of the Daqing River Basin, China. *Sustainability*, 13: 5626. DOI: [10.3390/su13105626](https://doi.org/10.3390/su13105626).
- Cui JQ, Broere W, Lin D. 2021. Underground space utilisation for urban renewal. *Tunnelling and Underground Space Technology*, 108: 103726. DOI: [10.1016/j.tust.2020.103726](https://doi.org/10.1016/j.tust.2020.103726).
- De Caro M, Crosta GB, Previati A. 2020. Modelling the interference of underground structures with groundwater flow and remedial solutions in Milan. *Engineering Geology*, 272: 105652. DOI: [10.1016/j.enggeo.2020.105652](https://doi.org/10.1016/j.enggeo.2020.105652).
- Dong L, Zhang J. 2021. Predicting polycyclic aromatic hydrocarbons in surface water by a multiscale feature extraction-based deep learning approach. *Science of the Total Environment*: 799. DOI: [10.1016/j.scitotenv.2021.149509](https://doi.org/10.1016/j.scitotenv.2021.149509).
- Foster S, Garduno H, Evans R, et al. 2004. Quaternary aquifer of the North China Plain — assessing and achieving groundwater resource sustainability. *Hydrogeology Journal*, 12: 81–93. DOI: [10.1007/s10040-003-0300-6](https://doi.org/10.1007/s10040-003-0300-6).
- Han JC, Huang Y, Li Z, et al. 2016. Groundwater level prediction using a SOM-aided stepwise cluster inference model. *Journal of Environmental Management*, 182: 308–321. DOI: [10.1016/j.jenvman.2016.07.069](https://doi.org/10.1016/j.jenvman.2016.07.069).
- He DF, Shan SQ, Zhang YY, et al. 2018. 3-D geologic architecture of Xiong'an New Area: Constraints from seismic reflection data. *Science China Earth Sciences*, 48(9): 1207–1222.
- Hu ZH, Li XZ, Zhao XB, et al. 2008. Numerical analysis of factors affecting the range of heat transfer in earth surrounding three subways. *Journal of China University of Mining and Technology*, 18: 67–71. DOI: [10.1016/S1006-1266\(08\)60015-2](https://doi.org/10.1016/S1006-1266(08)60015-2).
- Li HP, Wickham JD, Bushley K, et al. 2020. New approaches in urban forestry to minimize invasive species impacts: The case of Xiongan New Area in China. *Insects*: 11. DOI: [10.3390/insects11050300](https://doi.org/10.3390/insects11050300).
- Li R, Zhang J, Krebs P. 2021. Consumption- and income-based sectoral emissions of Polycyclic Aromatic Hydrocarbons in China from 2002 to 2017. *Environmental Science & Technology*, 55: 3582–3592. DOI: [10.1021/acs.est.0c08119](https://doi.org/10.1021/acs.est.0c08119).
- Li X, Ye SY, Wei AH, et al. 2017. Modelling the response of shallow groundwater levels to combined climate and water-diversion scenarios in Beijing-Tianjin-Hebei Plain, China. *Hydrogeology Journal*, 25: 1733–1744. DOI: [10.1007/s10040-017-1574-4](https://doi.org/10.1007/s10040-017-1574-4).
- Li XG, Yuan DJ. 2012. Response of a double-decked metro tunnel to shield driving of twin closely under-crossing tunnels. *Tunnelling and Underground Space Technology*, 28: 18–30. DOI: [10.1016/j.tust.2011.08.005](https://doi.org/10.1016/j.tust.2011.08.005).
- Liu FY, Cui JH, Chen LJ, et al. 2009. A view on geomorphologic zonalization of north china plain. *Geography and Geo-Information Science*, 25(4): 100–103.
- Ma Y, Li HQ, Zhang J, et al. 2020. Geophysical technology for underground space exploration in Xiongan New Area. *Acta Geoscientica Sinica*, 41(4): 535–542.
- Ma Z, Xia YB, Wang XD, et al. 2019. Integration of Engineering Geological Investigation Data and Construction of a 3D Geological Structure Model in the Xiong'an New Area. *Geo-*

- logy in China, 46: 123–138.
- Makungo R, Odiyo JO. 2017. Estimating groundwater levels using system identification models in Nzhelele and Luvuvhu areas, Limpopo Province, South Africa. *Physics and Chemistry of the Earth, Parts A/B/C*, 100: 44–50. DOI: [10.1016/j.pce.2017.01.019](https://doi.org/10.1016/j.pce.2017.01.019).
- Melaku ND, Wang J. 2019. A modified SWAT module for estimating groundwater table at Lethbridge and Barons, Alberta, Canada. *Journal of Hydrology*, 575: 420–431. DOI: [10.1016/j.jhydrol.2019.05.052](https://doi.org/10.1016/j.jhydrol.2019.05.052).
- Mengistu HA, Demlie MB, Abiye TA, et al. 2019. Conceptual hydrogeological and numerical groundwater flow modelling around the Moab Khutsong deep gold mine, South Africa. *Groundwater for Sustainable Development*, 9: 100266. DOI: [10.1016/j.gsd.2019.100266](https://doi.org/10.1016/j.gsd.2019.100266).
- Paris A, Teatini P, Venturini S, et al. 2010. Hydrological effects of bounding the Venice (Italy) industrial Harbor by a protection cutoff wall: Modeling study. *Journal of Hydrologic Engineering*, 15: 882–891. DOI: [10.1061/\(ASCE\)HE.1943-5584.0000258](https://doi.org/10.1061/(ASCE)HE.1943-5584.0000258).
- Qiao YK, Peng FL. 2016. Master planning for underground space in Luoyang: A case of a representative historic city in China. *Procedia Engineering*, 165: 119–125. DOI: [10.1016/j.proeng.2016.11.743](https://doi.org/10.1016/j.proeng.2016.11.743).
- Qin H, Cao G, Kristensen M, et al. 2013. Integrated hydrological modeling of the North China Plain and implications for sustainable water management. *Hydrology and Earth System Sciences*, 17: 3759–3778. DOI: [10.5194/hess-17-3759-2013](https://doi.org/10.5194/hess-17-3759-2013).
- Ricci G, Enrione R, Eusebio A, et al. 2007. Numerical modelling of the interference between underground structures and aquifers in urban environment. The Turin subway — Line 1. Available on <https://www.researchgate.net/publication/283166768>.
- Rwanga S, Ndambuki J. 2020. Solving groundwater problems fraught with uncertain recharge: An application to Central Limpopo, South Africa. *Groundwater for Sustainable Development*, 10: 100305. DOI: [10.1016/j.gsd.2019.100305](https://doi.org/10.1016/j.gsd.2019.100305).
- Sathe SS, Mahanta C. 2019. Groundwater flow and arsenic contamination transport modeling for a multi aquifer terrain: Assessment and mitigation strategies. *Journal of Environmental Management*, 231: 166–181. DOI: [10.1016/j.jenvman.2018.08.057](https://doi.org/10.1016/j.jenvman.2018.08.057).
- Serrano-Juan A, Pujades E, Vázquez-Suñé E, et al. 2018. Integration of groundwater by-pass facilities in the bottom slab design for large underground structures. *Tunnelling and Underground Space Technology*, 71: 231–243. DOI: [10.1016/j.tust.2017.07.020](https://doi.org/10.1016/j.tust.2017.07.020).
- Singha S, Pasupuleti S, Singha SS, et al. 2020. Effectiveness of groundwater heavy metal pollution indices studies by deep-learning. *Journal of Contaminant Hydrology*, 235: 103718. DOI: [10.1016/j.gsd.2019.100245](https://doi.org/10.1016/j.gsd.2019.100245).
- Uddin MG, Moniruzzaman M, Quader MA, et al. 2018. Spatial variability in the distribution of trace metals in groundwater around the Rooppur nuclear power plant in Ishwardi, Bangladesh. *Groundwater for Sustainable Development*, 7: 220–231. DOI: [10.1016/j.gsd.2018.06.002](https://doi.org/10.1016/j.gsd.2018.06.002).
- Wang C, Masoudi A, Wang M, et al. 2021. Land-use types shape soil microbial compositions under rapid urbanization in the Xiong'an New Area, China. *Science of the Total Environment*, 777: 145976. DOI: [10.1016/j.scitotenv.2021.145976](https://doi.org/10.1016/j.scitotenv.2021.145976).
- Wang GL, Liu ZM, Chen H, et al. 2010. Compilation of technical methods for investigation and evaluation of groundwater resources. Beijing, Geological Publishing House.
- Wu Y. 2003. Mechanism analysis of hazards caused by the interaction between groundwater and geo-environment. *Environmental Geology*, 44: 811–819. DOI: [10.1007/s00254-003-0819-9](https://doi.org/10.1007/s00254-003-0819-9).
- Xie SL, Su YB, Xu WH, et al. 2019. The effect of habitat changes along the urbanization gradient for breeding birds: An example from the Xiong'an New Area. *PeerJ*, 7(10): 7961. DOI: [10.7717/peerj.7961](https://doi.org/10.7717/peerj.7961).
- Xu HQ, Wang MY, Shi TT, et al. 2018. Prediction of ecological effects of potential population and impervious surface increases using a remote sensing based ecological index (RSEI). *Ecological Indicators*, 93: 730–740. DOI: [10.1016/j.ecolind.2018.05.055](https://doi.org/10.1016/j.ecolind.2018.05.055).
- Xu YS, Shen SL, Du YJ, et al. 2013. Modelling the cutoff behavior of underground structure in multi-aquifer-aquitard groundwater system.

- Natural Hazards, 66: 731–748. Available on <https://link.springer.com/article/10.1007/s11069-012-0512-y>
- Xu YS, Ma L, Shen SL, et al. 2012. Evaluation of land subsidence by considering underground structures that penetrate the aquifers of Shanghai, China. *Hydrogeology Journal*, 20: 1623–1634. DOI: [10.1007/s10040-012-0892-9](https://doi.org/10.1007/s10040-012-0892-9).
- Yang W, Wang Z, Hua P, et al. 2021. Impact of green infrastructure on the mitigation of road-deposited sediment induced stormwater pollution. *Science of the Total Environment*: 770.
- Yang W, Zhang J. 2021. Assessing the performance of gray and green strategies for sustainable urban drainage system development: A multi-criteria decision-making analysis. *Journal of Cleaner Production*: 293. DOI: [10.1016/j.jclepro.2021.126191](https://doi.org/10.1016/j.jclepro.2021.126191).
- Zhu X, Wang G, Wang X, et al. 2022. Hydrogeochemical and isotopic analyses of deep geothermal fluids in the Wumishan formation in Xiong'an New Area, China. *Lithosphere*: 2021.
- Zou WY, Yin SQ, Wang WT. 2021. Spatial interpolation of the extreme hourly precipitation at different return levels in the Haihe River basin. *Journal of Hydrology*, 598: 126273. DOI: [10.1016/j.jhydrol.2021.126273](https://doi.org/10.1016/j.jhydrol.2021.126273).